GMR
The Original

IN SILICO EVALUATION OF ANTIVIRAL POTENTIAL OF EMBLICA OFFICINALIS PHYTOCONSTITUENTS TARGETING CHIKUNGUNYA VIRUS NSP3 PROTEIN

Ripu Daman[1]*, Monika Miglani[2]

[1*]Department of Biotechnology, Chaudhary Bansi Lal University, Bhiwani, 127031, Haryana, India
[2]Centre for Bioinformatics, Maharshi Dayanand University, Rohtak, 124001, Haryana, India, drmonikamiglani@gmail.com, https://orcid.org/0000-0003-0298-0252
*Corresponding Author: Email: drmonikamiglani@gmail.com, ORCID: https://orcid.org/0000-0003-3003-7026

ABSTRACT
Chikungunya virus (CHIKV), an emerging arbovirus belonging to the genus Alphavirus (family Togaviridae), poses a significant global health challenge due to the absence of specific antiviral therapeutics. The present study investigates the antiviral potential of phytoconstituents from Emblica officinalis against the non-structural protein 3 (nsP3), a key component involved in viral replication, using in silico approaches. A set of selected phytochemicals was screened through molecular docking using AutoDock, followed by pharmacokinetic evaluation via ADMET analysis. Among the compounds, alpha-carotene, beta-sitosterol, kaempferol, and lupeol exhibited notable binding affinities toward the nsP3 protein. Interaction analysis indicated that hydrophobic interactions predominantly contributed to ligand binding. Furthermore, molecular dynamics simulation of the top-ranked complex demonstrated structural stability, with minimal conformational deviations observed over a 100 ns simulation period. These findings suggest that bioactive compounds from E. officinalis may serve as promising candidates for the development of anti-CHIKV therapeutics. However, further experimental validation is required to confirm their efficacy and safety.

KEYWORDS: Chikungunya virus, nsP3 protein, Emblica officinalis, Molecular docking, Phytoconstituents

• INTRODUCTION

Chikungunya virus (CHIKV) belongs to the genus Alphavirus within the Togaviridae family. It was discovered firstly in Tanzania in 1952 (Strauss et al., 1986). The name Chikungunya is obtained from the Makonde word which describes a stooped position seen during acute illness in patients with high degree of arthralgia (Mavalankar et al., 2008). In the last fifty years, outbreaks of CHIKV have been observed mostly in East and South Africa (Novillo et al., 2016). The global burden of chikungunya (by CHIKV) disease has significantly increased in recent years (Weaver et al., 2015, Silva et al., 2017). The increasing magnitude and dissemination from Africa to Asia, America, and the Europe is an indicator of its emergence as a public health concern across the globe. In 2005, CHIKV re-emerged in India, infecting approximately 1.4 million people across various states and causing significant losses in productivity and economic value. By 2015, 23 states had reported cases of chikungunya fever (CHIKF), and by 2019, the virus had spread to nearly all states. CHIKV data showed 2368 confirmed cases were reported in India till November 2025. While new cases have emerged in many states, Maharashtra, Karnataka, and Tamil Nadu continue to report the highest numbers (Shanmugaraj et al., 2026).This trend reflects the current high epidemiological burden and requirement for effective control measures. Humans are mainly infected by the bite of mosquito, primarily through Aedes aegypti and Aedes albopictus (Schuffenecker et al., 2006). CHIKV genome consists of a single stranded 12 kb RNA with a 3′ poly (A) tail and a 5′ cap. The majority of the genetic material codes for four nonstructural proteins (nsP1–nsP4), which are important in transcription and viral replication (Ferreira et al., 2021). The last third is a subgenomic RNA that encodes the structural proteins required for virion assembly and subsequent infection. CHIKV virions are spherical particles approximately 70 nm in diameter (Zaid et al., 2018). The infection can be diagnosed in the laboratory using serological assays, virus extraction, and cDNA amplification assays (Ali et al., 2012). The mode of treatment for Chikungunya is mostly symptomatic. However if nonsteroidal anti-inflammatory drug (NSAID) therapies fail, methotrexate, sulfasalazine, and hydroxychloroquine are used as antirheumatic disease-modifying drugs (DMARDs). This is especially true for cases that progress to chronic inflammatory arthritis (Metz et al., 2013). Analgesics are used as an adjunctive treatment for severe joint pain. However, no specific antiviral agents have been approved for CHIKV (Thiberville et al., 2013), and current therapeutic strategies rely mostly on supportive care, which has limited effectiveness against viral replication. In this regard, plant-based pharmacotherapeutics have attracted much interest as promising alternatives. Various phytochemicals like flavonoids, alkaloids, terpenoids, and polyphenols have been demonstrated to inhibit the virus by disrupting its process of entering the cells, replication, and assembly (Hamed et al., 2019; Newman et al., 2020). Nevertheless the classical laboratory based approaches for evaluating their binding potential and activity are labor-intensive and cost-inefficient (Sen et al., 2014). Open-source bioinformatics tools and inexpensive computing power have greatly accelerated in silico drug discovery. One such method to find

possible hits quickly and efficiently is in silico screening by computer-aided molecular docking techniques that predict the interaction between candidate ligands and target macromolecules (Trott et al., 2016). Nevertheless, both animal models and human clinical trials are essential for assessing therapeutic activity and safety (Vora et al., 2020). However, in vitro testing needs to be used for further validation. Although CHIKV non-structural proteins have been widely investigated, the majority of antiviral strategies mainly target enzymatic components nsP2 (protease/helicase) and nsP4 (RNA-dependent RNA polymerase). Nevertheless, nonstructural protein 3 (nsP3) has proved to be a central regulator of the viral replication complex. Given the interactions of this protein with several host cellular factors (Rodriguez et al., 2024), it is not surprising that it has shown importance during replication, both in organizing and stabilizing the entire restructuring process. On the other hand, nsP1 and nsP4 more strictly perform enzymatic functions than structural regulatory roles. A remarkably flexible hypervariable region and a macro-domain conserved among all arboviruses implicated in ADP-ribose binding enable nsP3 to manipulate host antiviral pathways that are crucial for viral replication and pathogenesis. Due to its multiple roles, nsP3 is an important determinant of virus pathogenicity. Furthermore, in contrast to other nonstructural proteins, there has been a lack of studies targeting nsP3 as a therapeutic target in novel antiviral drugs from plants. Consequently, the attention towards nsP3 opens a new avenue for potential antiviral drug discovery against CHIKV (Rallabandi et al., 2020).

The Emblica officinalis plant is widely known for its phytochemical profile. It possess a number of pharmacological properties, including antioxidant, antiviral, antidiabetic, hypolipidemic, and antibacterial activities. It has long been used to treat various diseases; therefore, it is a high source of compounds that are bioactive for the new generation of antiviral medications (Gaire et al., 2014). To identify potential lead compounds, the present study employs a structure-oriented strategy to computer based ligand design, wherein a virtual library of phytochemicals obtained from Emblica officinalis is generated and systematically screened. The study involves the computational evaluation of binding affinity for individual shortlisted phytochemicals against the CHIKV nsP3 protein using molecular docking. ADMET analysis predicts pharmacokinetic and toxicity profiles, along with evaluating drug-likeness characteristics. Molecular modeling is also employed to assess the kinetics and structure of ligand–protein conjugates in a quinary system. In conclusion, our initial study provides a framework for plant-based antiviral drug discovery through phytochemical screening through combination of advanced computational approaches to discovering viable, safe and cost-effective therapeutic leads against CHIKV infection.

2. MATERIALS AND METHODS

2.1 Phytochemical database generation

A phytochemical database of 20 biological metabolites of Emblica officinalis was generated using a systematic literature mining and used in the current study (Table 1). Relevant compounds with known pharmacological and antiviral properties were identified from publications accessed using scientific databases (PubMed, Google Scholar). Selected compounds were packaged and prepared for further computational analysis (Ashfaq et al., 2013).

2.2 Preparation of Target Protein and ligand

The molecular structural organisation of Chikungunya virus nonstructural protein 3 (nsP3) with additional three extra dimensions was retrieved from RCSB PDB (PDB ID: 3ZTB). The preprocessing of the protein was done with the help of using AutoDock Tools (version 1.5.7). Initially, the heteroatoms and crystallographic molecules of waters were deleted from the two structures, missing hydrogen atoms were included. It then received AD4 atom types and Kollman unified atom charges. Finally, the processed protein conformation was exported to PDBQT arrangement for subsequent molecular interaction analyses (Dutta et al., 2005). The three-dimensional structures of the selected phytochemicals were retrieved from the PubChem library (Kim et al., 2021). Ligand preparation was performed using ADT interface (version 1.5.7). Each ligand was adjusted to minimized energy and geometrically optimized configuration to obtain a stable conformation for molecular docking. Partial charges (Gasteiger) were subsequently applied and polar hydrogen atoms added. Then, the compounds were executed and saved in format PDBQT for subsequent docking studies (Kim et al., 2021). Similarly, Abacavir drug (which was included as positive control to confirm the docking protocol and provide comparative reference on binding affinity) was prepared for molecular docking.

2.3 Drug-Likeness and ADME Analysis

The absorption, distribution, metabolism, and excretion (ADME) properties of the selected phytochemicals were evaluated using the SwissADME web server (https://www.swissadme.ch/), a freely accessible online platform for predicting physicochemical characteristics, pharmacokinetic parameters, drug-likeness, and medicinal chemistry friendliness of bioactive compounds. Since herbal therapeutic agents may exhibit undesirable side effects despite their natural origin, assessment of their pharmacokinetic behavior is essential during the drug discovery process.

The ADME analysis included evaluation of gastrointestinal absorption (GIA), blood–brain barrier permeability (BBBP), drug-likeness, bioavailability, and other pharmacokinetic parameters. Drug-likeness was assessed based on established rules, including Lipinski's Rule of Five, to determine the suitability of the compounds as potential orally active drug candidates. The obtained results were used to identify compounds with favorable pharmacokinetic profiles and acceptable drug-like characteristics for further investigation.

2.4 Active site prediction

Active site prediction of the proteins were analyzed using the online web server PrankWeb. According to PrankWeb predicted result, the active site present on NSP3 Protein of Chikungunya virus is (ASP10, ILE11, ALA22, ASN24,

VAL33, LEU108, SER110, GLY112, THR111, TYR114, ARG144, ASP145, and TRP148). The binding site was used to point out how to analyze the Grid Box and docking.

2.5 Molecular Docking

In silico molecular interaction analysis were demonstrated to evaluate the nsP3 protein interacting affinities and interaction profiles of plant metabolites using AutoDock Tools program (version 4.2.6) (Morris et al., 2009). However, the conformational space of the ligand was rapidly explored (Powers et al., 2015) using AutoDock's Lamarckian GA optimization (Morris et al., 1998). For the reliability of docking procedure Abacavir was docked in similar conditions and its binding affinity was also used as a reference to measure the Phytochemicals. The best binding conformations were determined in terms of the lowest affinity energy (kcal/mol) and related inhibition constant (Ki). The conformation that had the lowest energy was selected for further examination for each of the examined molecules (Feinstein et al., 2015).

2.5.1 Grid Box Configuration

The grid box for nsP3 was generated to cover the active amino acid residues involved in ligand binding. The grid dimensions were set at 126 × 126 × 126 points with a grid spacing of 0.375 Å. The grid box was centered at the selected binding region to ensure complete coverage of the active site and surrounding residues for molecular docking studies. These parameters were chosen to facilitate accurate prediction of ligand–protein interactions and binding affinities. The grid box size for nsP3 (size_x = 126 size_y = 126 size_z = 126 and grid-centered at X, Y, and Z coordinates of respectively) was used to cover active amino acid residues for docking.

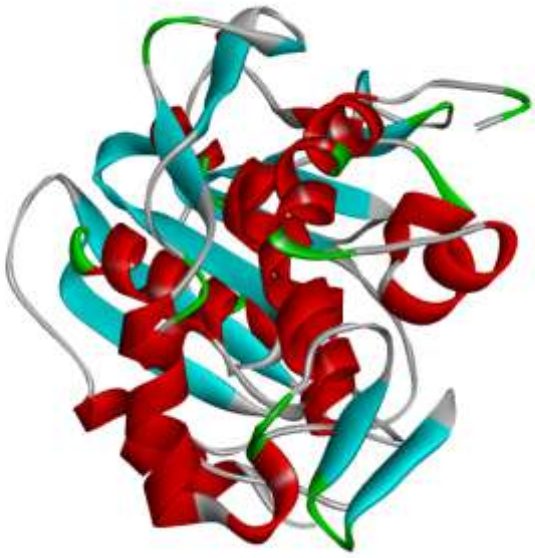

Fig1. Crystal structure of CHIKV Proteins, NSP3 Protein was taken from Protein Data Bank (PDB) and visualized with the help of BIOVIA Discovery Studio Visualizer software.

2.5.2 Docking Specifications

Docking simulations were performed using the following configurations at 50 independent runs in total, size of generation: 300, Max energy evaluations: 2.5×10^{n} and the initial values of other variables were preserved.

2.6 Protein–Ligand Interaction Assessment

The predicted complexes of protein–ligand were analyzed through Discovery Studio Visualizer (version 20.1). Includes interacting interaction plots in two (2D) and three (3D): the shell significant binding affinities in active site, hydrogen bonds, hydrophobic interactions, π–π stacking and crystal noncovalent contacts.

2.7 Molecular dynamics simulation study

To perform a simulation study and analyze the dynamic properties and structural rigidity of selected macromolecule–ligand complexes, we used the Desmond module (Bowers et al., 2009) (Schrödinger LLC). These are complexes where docked or user original arrangements were transformed. This was with an explicit solvent model (TIP3P water model) allocated within the orthorhombic simulation box, and appropriate counter ions inserted to counter the charge of the system. It was done with the intent to lower the energy prior to the production run.

NPT ensemble simulations were undertaken for a total of 100 ns at temperature = 310 K and pressure =1 atm. Interatomic relationships were modeled using the OPLS molecular mechanics force field. Post-simulation trajectory analyses were used to evaluate structural deviation (RMSD) for structural integrity, structural fluctuations (RMSF) for residue adaptability analysis, overall binding reliability and conformational dynamics of the molecules across the active sites (Binder et al., 2004).

- **RESULTS**

The molecular docking analysis revealed that the bioactive phytochemicals of Emblica officinalis exhibited varying degrees of binding affinity toward the Chikungunya virus nsP3 protein, with docking scores ranging from −3.81 to −11.22 kcal/mol. Among the tested compounds, α-carotene demonstrated the strongest binding affinity (−11.22 kcal/mol), followed by β-sitosterol (−8.42 kcal/mol), oleanolic acid (−8.36 kcal/mol), lupeol (−8.14 kcal/mol), kaempferol (−7.72 kcal/mol), and quercetin (−7.31 kcal/mol). Notably, several phytochemicals displayed better binding affinities than the reference antiviral drug Abacavir (−6.63 kcal/mol). The ligand–protein complexes were stabilized through interactions with key amino acid residues, including Ser, Trp, Tyr, Lys, Pro, Met, and Ala, involving hydrophobic contacts, hydrogen bonds, and van der Waals interactions. These findings suggest that the selected phytochemicals possess significant binding potential against the nsP3 protein and may serve as promising candidates for the development of anti-Chikungunya therapeutics. The detailed interaction profiles are illustrated through two-dimensional (2D) and three-dimensional (3D) docking representations shown in Figure 1.

3.1 Molecular Docking Analysis

Molecular interaction was done in silico to elucidate the binding energy as well as binding modes of 20 bioactive phytochemicals from Emblica officinalis with nsp3. Results indicated a wide array of binding energies, with different ligand–protein complexes exhibiting varying degrees of interaction and stability.

Table 1. Binding efficiency of plant compounds with the docked target protein Nsp3.

S.No.	Compound	CID	Binding energy kcal/mol	Interactive residue
1.	Alpha carotene	6419725	-11.22	ALA8, ASN9, CYS11, TRP12, ALA44, TYR45, SER46, TYR77, ASN80, HIS81, TRP82, LEU203, GLN239, MET240, ARG269, VAL270, VAL273
2.	Ascorbic acid	54670067	-3.92	GLY112, VAL33, TYR114
3.	Astragalin	5282102	-5.64	ASN24, ALA22, TYR114, TRP148, MET87, TRP148, GLY112, ASP145, LEU108, SER110, TYR114
4.	Ellagic acid	5281855	-6.64	LEU108, ASN24, TYR114, SER110, PRO132, ASP145, GLY112.
5.	Beta sitosterol	222284	-8.42	SER110, TRP148, CYS34, ALA22, MET87, GLY112.
6.	Chebulic acid	71308174	-5.90	GLN21, ARG144, THR111, LYS118.
7.	Corilagin	73568	-4.96	GLN21, ARG144, THR111, LYS118, ASP145, SER110.
8.	Galactaric acid	3037582	-4.75	ALA22, HIS37, GLU13, ILE11, ASN24, THR111.
9.	Furosin	10416810	-4.65	THR111, VAL33, GLU13, MET87, ARG144, LEU108.
10.	Gallic acid	370	-5.14	SER110, TRP148, TYR114, TRP148, CYS34, ASN24.
11.	Kaempferol	5280863	-7.72	SER110, TRP148, TYR114, ASN24, ALA22.
12.	Leucodelphidin	440835	-6.19	ILE11, HIS37, TYR114, TRP148, VAL33, ASN24.
13.	Linoleic acid	5280450	-6.64	LYS118, GLU13, MET87, LEU108, PRO132.
14.	Quercetin	5280343	-7.31	SER110, THR111, LYS118.
15.	Lupeol	259846	-8.14	GLY112, ALA22, LEU108, PRO132, MET87, TYR114.
16.	Nicotinic acid	938	-3.81	PHE114, SER110, MET87.
17.	Nitric acid	944	-6.05	ALA22, GLN21, ASP145.
18.	Oleanolic acid	10494	-8.36	LYS118, ILE11, PRO132.
19.	Myristic acid	11005	-6.02	GLU13, ALA22, ASP145, GLN21, GLU13, TYR114.
20.	Oleic acid	445639	-5.86	LYS118, ILE11, MET87.

The normally-used, anti-viral drug Abacavir was furthermore utilized as optimistic control for all evaluation and was revealed to have a binding affinity of −6.63 kcal/mol (Table 2). Out of the selected, αcarotene (CID: 6419725) has the

highest binding affinity with molecular interaction energy score −11.22 kcal/mol and demonstrated stable & significant interaction in active sites of nsP3 (Table 1). The most of the hydrophobic affinities observed in the conformational binding of α-carotene were due to amino acid residues near and on the site, suggesting that they facilitated greater stability in the complex (Meng et al., 2011; Rasool et al., 2021).

Table 2. Binding efficiency of Drug Abacavir with the docked target protein Nsp3.

S.No.	Compound	CID	Binding energy kcal/mol	Interactive residue
1.	Abacavir	441300	-6.63	SER110, TRP148, TYR114, ASN24**.**

Other high-affinity compounds of note were β-sitosterol (−8.42 kcal/mol), oleanolic acid (−8.36 kcal/mol), and lupeol (−8.14 kcal/mol). The aforementioned compounds associated mainly with residues like Ser, Trp, Cys, and Met, suggesting stabilization through hydrophobic contacts and van der Waals forces. The presence of interactions between Lys, Ile, and Pro residues along with these hydrophobic amino acid residues indicates a probable combination of hydrophobic and electrostatic interactions between the enzyme receptor and oleanolic acid. Lupeol also established stable interactions with residues Gly, Ala, Leu, Pro, Met, and Tyr in the binding pocket (Rahman et al., 2021). Moreover, kaempferol (-7.72 kcal/mol) exhibited a moderate binding energy due to a combination of hydrogen and hydrophobic interactions (Ferreira et al., 2015). It associated with amino acids such as Ser, Trp, Tyr, Asn, and Ala. Compared to highly hydrophobic ligands, it exhibited a more balanced interaction profile, which included polar interaction (Table 1).

These docking results indicate that hydrophobic interactions are the most significant stabilizing forces in ligand binding to the nsP3 active site, while hydrogen bonds make the main contribution to binding affinity and the adequate orientation of the ligand. Figure 1 showing Two-dimensional (2D) and three-dimensional (3D) interaction profiles of phytochemicals with the Chikungunya virus nsP3 protein and it is explained by variations in molecular docking, polarity, and structural complementarity with the binding pocket.

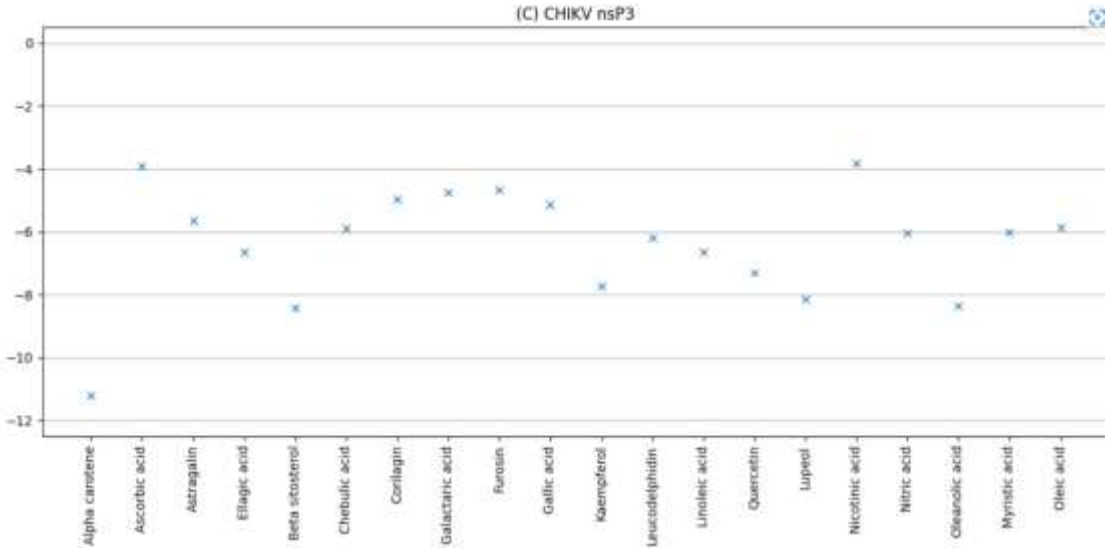

Fig. 2 Graphical representation of binding energy of ligands with different proteins.

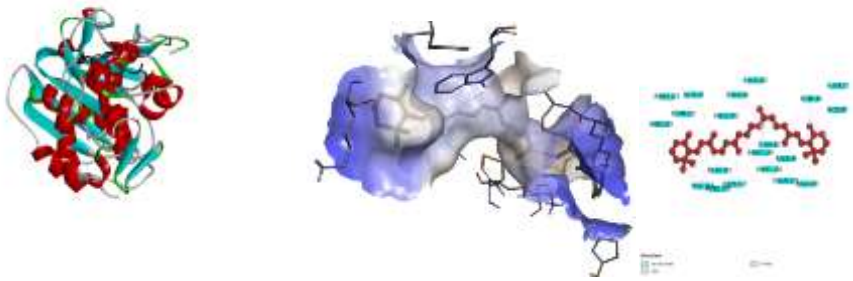

Fig 1. (i) 3-D and 2-D interaction of Alpha carotene with Nsp3 protein .

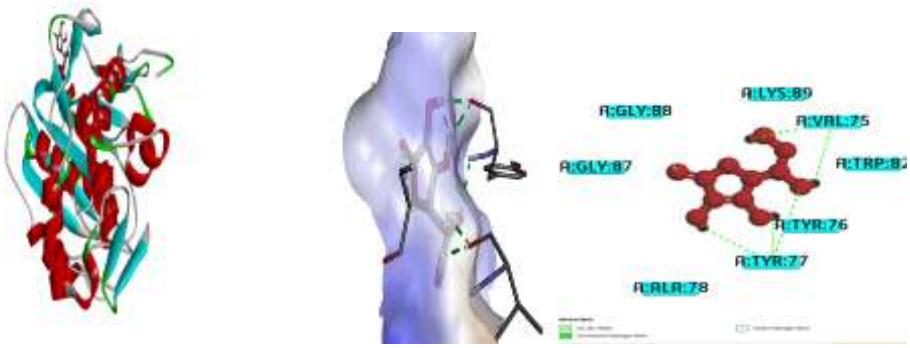

(ii) 3-D and 2-D interaction of Ascorbic acid with Nsp3 protein.

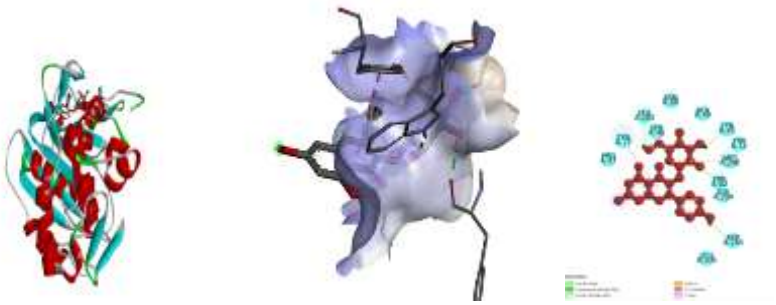

(iii)3-D and 2-D interaction of Astragallin with Nsp3 protein.

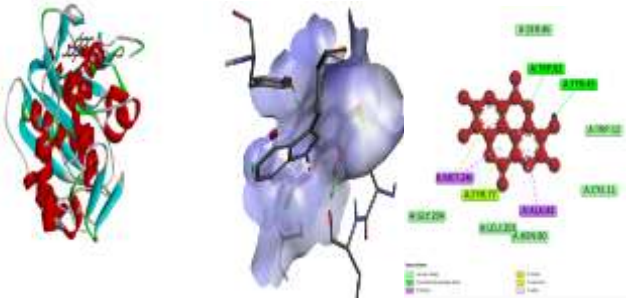

(iv) 3-D and 2-D interaction of Benzoaric acid with Nsp3 protein.

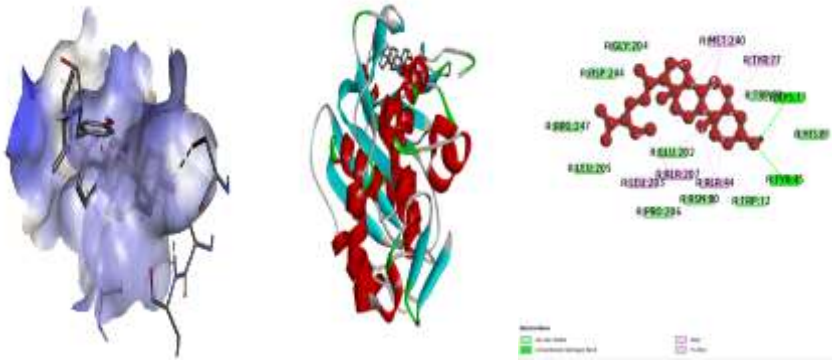

(v) 3-D and 2-D interaction of Beta-sitosterol with Nsp3 protein.

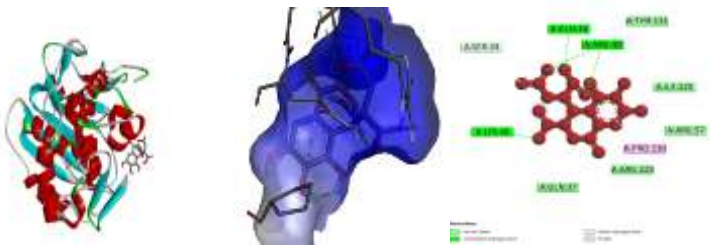

(vi) 2-D interaction of chebulic acid with Nsp3 Protein.

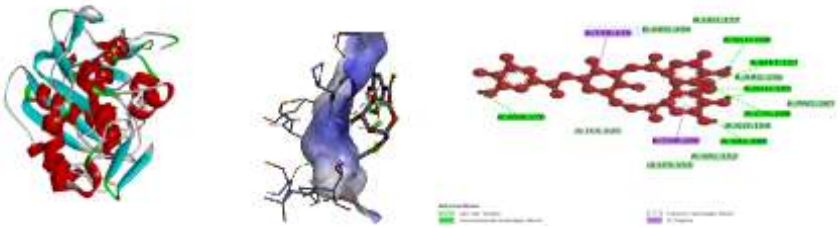

(vii) 3D and 2-D interaction of Corillagin with Nsp3 protein.

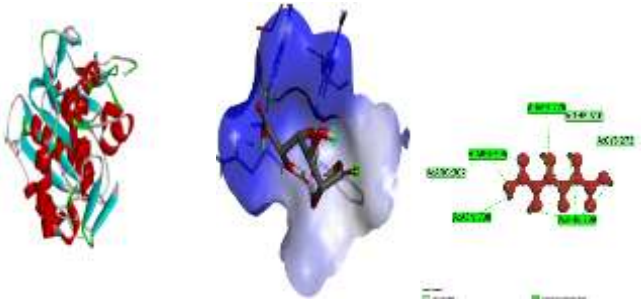

(viii) 3-D and 2-D interaction of galactaric acid with Nsp3 protein.

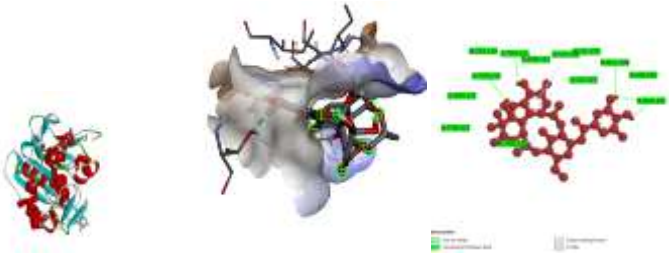

(ix) 3-D and 2-D interaction of Furosin with Nsp3 protein.

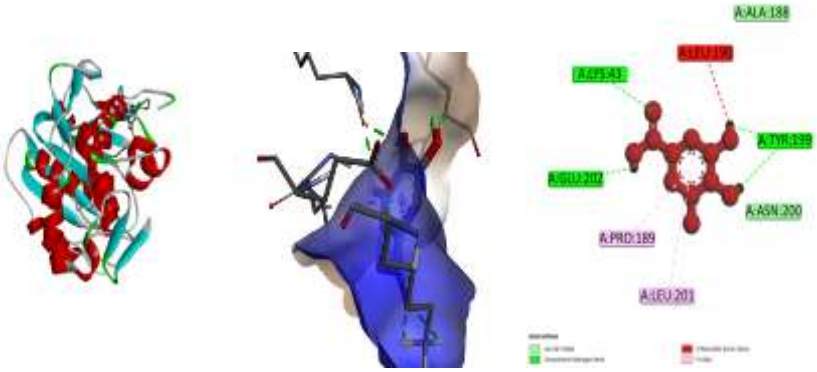

(x) 3-D and 2-D interaction of gallic acid with Nsp3 protein.

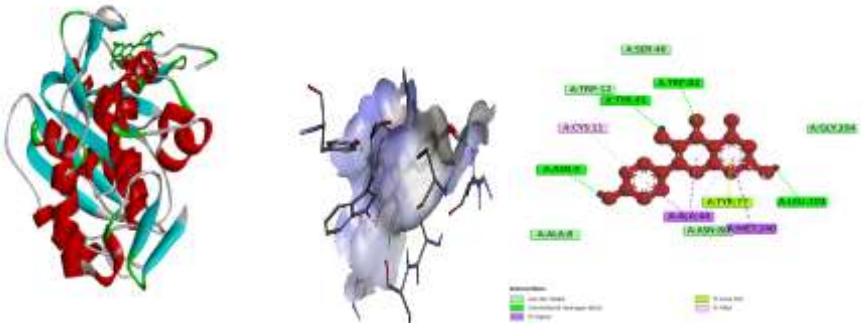

(xi) 3-D and 2-D interaction of Kaempferol with Nsp3 protein.

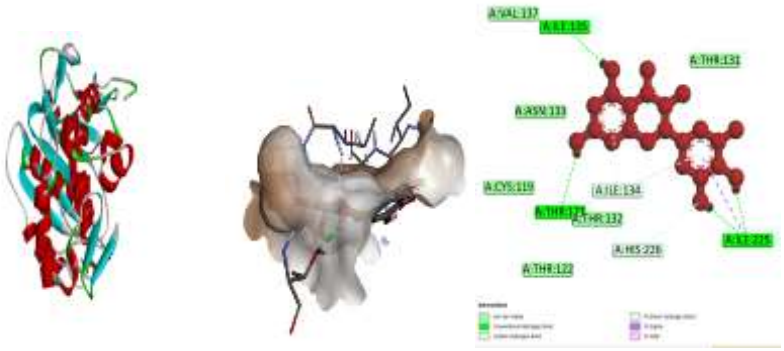

(xii) 3-D and 2-D interaction of Leucodelphidin with Nsp3 protein.

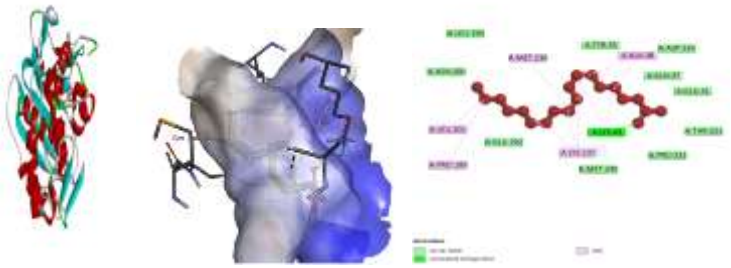

(xiii) 3-D and 2-D interaction of Linoleic acid with Nsp3 protein.

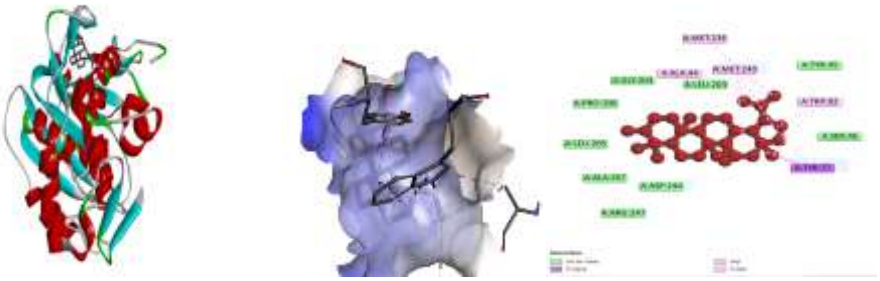

(xiv) 3-D and 2-D interaction of Lupeol with Nsp3 protein.

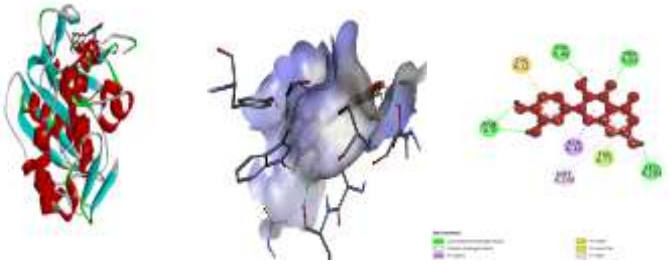

(xv) 3-D and 2-D interaction of Quercetin with Nsp3 protein.

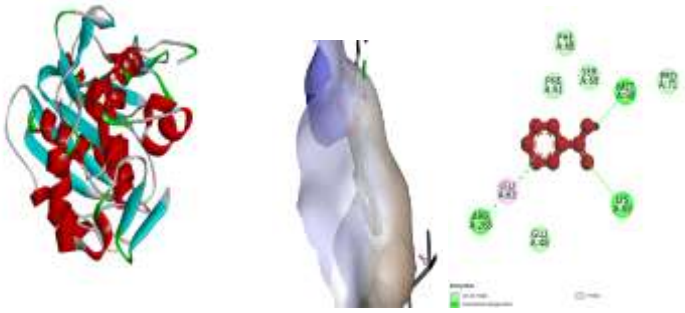

(xvi) 3-D and 2-D interaction of Nicotinic acid with Nsp3 protein.

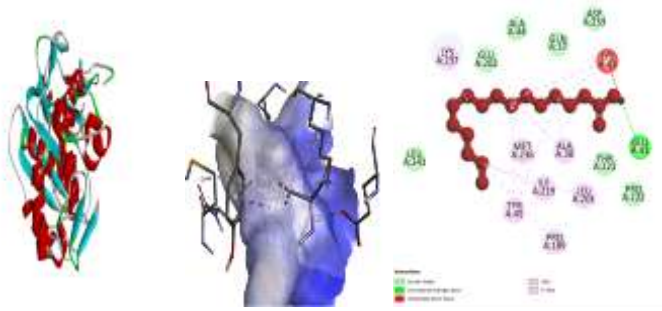

(xvii) 3-D and 2-D interaction of Nitric acid with Nsp3 protein.

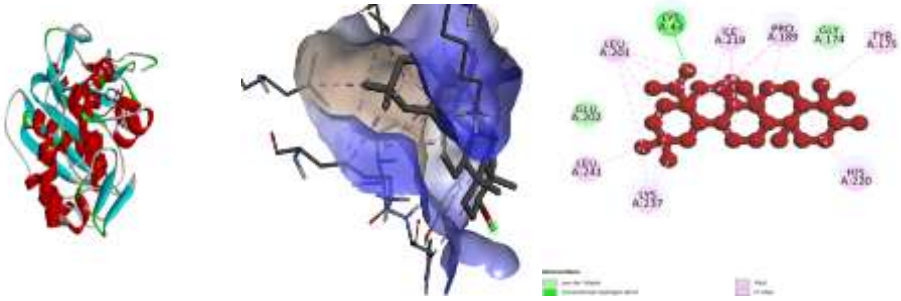

(xviii) 3-D and 2-D interaction of Oleanolic acid with Nsp3 protein.

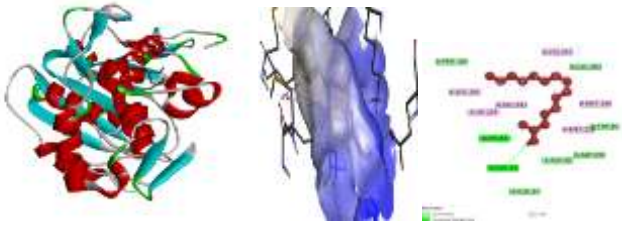

(xix) 3-D and 2-D interaction of Myristic acid with Nsp3 protein.

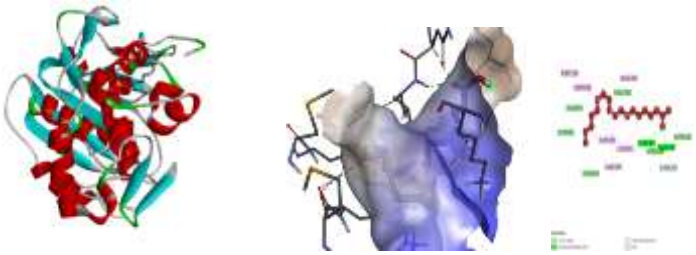

(xx) 3-D and 2-D interaction of Oleic acid with Nsp3 protein.

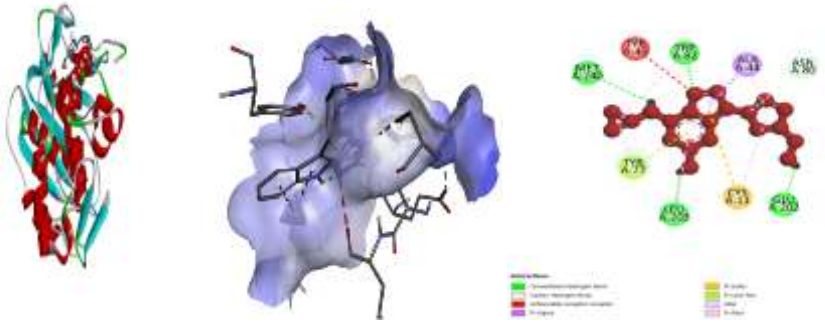

(xxi) 3-D and 2-D interaction of Abacavir drug with Nsp3 protein.

Figure 1. Showing Two-dimensional (2D) and three-dimensional (3D) interaction profiles of phytochemicals with the Chikungunya virus nsP3 protein:
(i) α-carotene, (ii) ascorbic acid, (iii) astragalin, (iv) benzoic acid, (v) β-sitosterol, (vi) chebulic acid, (vii) corilagin, (viii) galactaric acid, (ix) furosin, (x) gallic acid, (xi) kaempferol, (xii) leucodelphidin, (xiii) linoleic acid, (xiv) lupeol, (xv) mucic acid, (xvi) nicotinic acid, (xvii) nitric acid, (xviii) oleanolic acid, (xix) myristic acid, and (xx) oleic acid.

3.2 Molecular Dynamics Simulation Analysis

To further assess the accuracy of binding interactions, molecular dynamics simulation was also performed on the best-scoring complex (α-carotene–nsP3) for a 100 ns trajectory under physiologically relevant conditions. The root mean square deviation (RMSD) of the peptide backbone sharply increased during the equilibration stage (0–20 ns) and subsequently fluctuated around 2.2 Å with a plateau between 2.4 Å (Sharma et al., 2021). This phase relates to structural relaxation and adaptation from the docked state. The RMSD stabilized to approximately 1.6–2.0 Å after equilibration, indicating that the ligand-protein complex was stable and converged. In contrast, the ligand RMSD was relatively more variable, with values in the range of about 1.0–3.8 Å, indicating comformational flexibility of the ligand inside the binding site, which did not affect the stability of the total interaction of each specific ligand bound to the protein. Specifically, we observed that the ligand RMSD converged after 30 ns of simulation (Karplus et al., 2002) and showed only minor fluctuations, suggesting that the ligand was well accommodated in the active site with slight displacement. Caveats in interfering binding modes can include occasional shifts due to transient conformational rearrangements or localized flexibility of residues involved in the binding region (Azmal et al., 2024). The ligand-protein complex showed an RMSD profile that suggested a dynamic interaction of nsP3 (Fig. 4 (i)) (Durrant et al., 2011), indicating that nsP3 had stable dynamic binding with α-carotene. Another confirmation of the docking results was the absence of any major structural changes, and the ligand remaining in the binding pocket (5→6).

The RMSF profile shows moderate fluctuations across most residues, indicating overall structural stability of the protein during the simulation.

Higher peaks observed at specific residue regions suggest localized flexibility, likely corresponding to loop or surface-exposed regions.

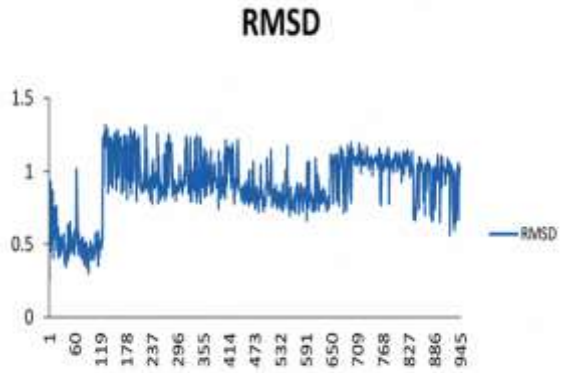

Fig2.1. The figure represents the Root Mean Square Deviation (RMSD) profile of the protein–ligand complex over the course of the molecular dynamics simulation.

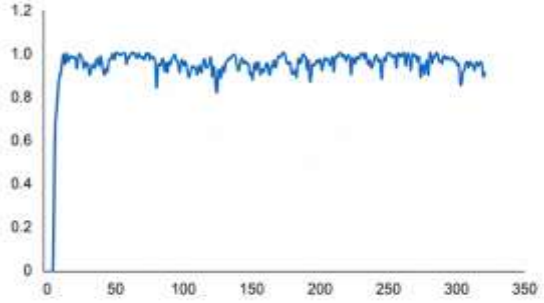

Fig2.2. The figure illustrates the Root Mean Square Deviation (RMSD) trajectory of the protein–ligand complex during the molecular dynamics simulation, providing insight into its structural stability over time.

In addition to RMSD and RMSF calculations, Rg and SASA profiles were employed to independently calculate the structural strength of the nsP3–ligand complex. The Rg plot suggested that the protein's structure was compact across the 100 ns simulation thus indicating no considerable unfolding or any expansion on binding of ligand. This indicates that proteins are dynamic in the physiological conditions as apparent from these small variations of Rg values.

Likewise, SASA analysis indicates that there were only minor fluctuations of the protein throughout the entire duration of simulation, pointing towards a relatively constant solvent exposure. This means that there were no significant conformational variations upon ligand association, and that the protein structure did not lose its integrity. Additionally, the lack of large SASA changes further supports that ligand remained stably buried within hydrophobic binding pocket without leading to major surface exposure changes.

Collectively, the stable Rg and SASA (Fig. 2.(iii) profiles verified the findings of RMSD, indicating that nsP3–α-carotene complex is capable of retaining structural stability and compact throughout the simulation time.

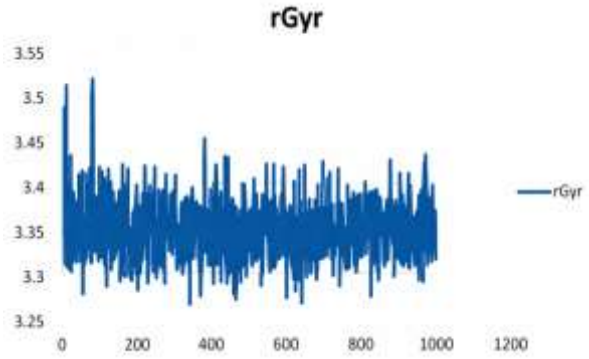

Fig2.3. The figure shows the Radius of Gyration (rGyr) profile of the protein–ligand complex throughout the molecular dynamics simulation, which reflects the overall compactness and structural folding of the system.

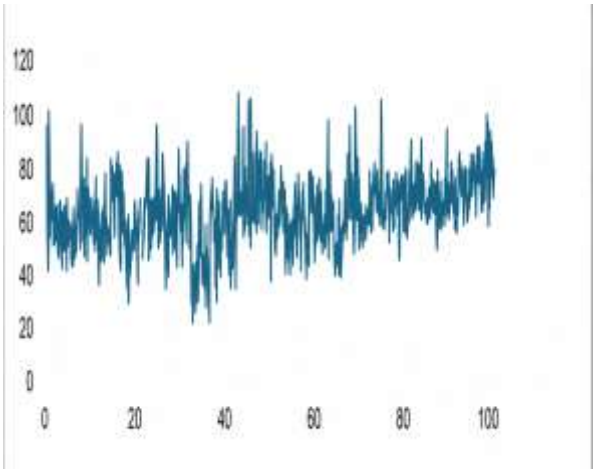

Fig 2.4. The figure represents the Solvent Accessible Surface Area (SASA) of the protein–ligand complex over.

the course of the molecular dynamics simulation, which provides insight into the extent of surface exposure of the biomolecule to the solvent.

Fig. 2. Multiple MD simulations: Stability analysis of the CHIKV nsP3 macrodomain with phytocompound having highest binding efficiency i.e. Alpha carotene. Among all the interactions recorded, we measured the (i) nsP3-ligand hydrogen bond's number over time and found that only 0.89% corresponded to an intramolecular hydrogen bond within the ligand itself, indicating that binding stability is governed mainly by hydrophobic contacts. (ii) Radius of gyration (Rg) did not change significantly during the simulation, suggesting that overall nsP3 firmness was fairly maintained after binding to ligand. (iii) Solvent accessible surface area (SASA) analysis presented slight variations in SASA values of protein during 1000ps. MD simulations time points, indicating that there were no significant expansion or collapse conformation and supporting the strength of the docked complex.

Also the molecular dynamics simulation of reference drug Abacavir–nsP3 complex is generate under same simulation condition to confirm the stability of phytochemical complexes. The Abacavir–nsP3 RMSD profile exhibited an initial equilibration phase in the first 15–20 ns, and then plateaued to values around 1.8–2.5 Å for the remaining time points simulated. While the complex showed moderate fluctuations, RMSD values were higher and more remote than compared to α-carotene–nsP3 indicating a comparatively decreased stability of the Abacavir-bound system (Azmal et al., 2024).

Analogous to RMSF profile of Abacavir complex, the Abacavir RMSF profile showed significant residue-level flexibility across the whole working protein with some evidence of localized structural fluidity in loop-region conformations. In contrast, the docked phytochemicals α-carotene, β-sitosterol, oleanolic acid and lupeol remained in relatively less variable toroidal domains among the active residues implying greater stabilization within its hydrophobic binding pocket.

Over the course of the simulation, Rg values for the Abacavir-bound nsP3 complex remain relatively stable at ~2.08–2.16 nm (evidence of protein compactness). In comparison to the phytochemical complexes only smaller oscillations were observed but they suggest slightly less compact stability. Similarly, SASA analysis revealed a more moderate degree of fluctuation for the Abacavir complex suggesting periodic differences in surface solvent exposure whereas the top phytochemical ranked complexes had stable SASA profiles providing evidence of a stronger structure (Lobanov et al., 2008).

Hydrogen bond (H-bond) analysis also indicated that Abacavir–nsP3 complex established transient hydrogen bonds between 0–3 on simulation trajectory. While these interactions assisted in stabilization, the persistences and occupancies of hydrogen bonds were relatively lower than those within selected phytochemical complexes, where hydrophobic mediators contributed the most to ligand stability.

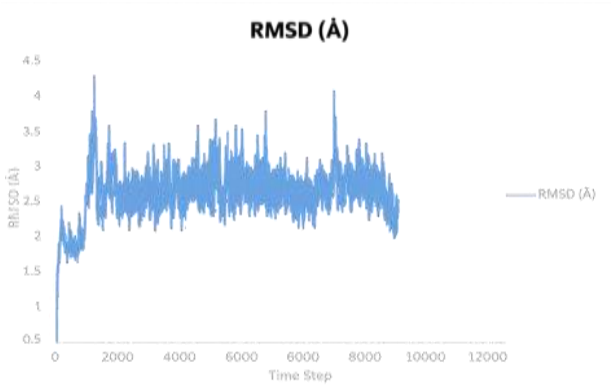

Fig.3.1. Fig. 4.1. **RMSD analysis of the Abacavir–nsP3 complex showing structural deviations and overall stability throughout the simulation trajectory.**

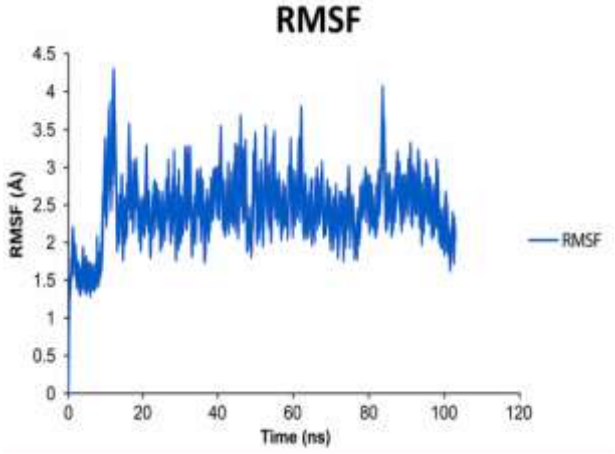

Fig.3.2. RMSF profile of the Abacavir–nsP3 complex indicating residue-wise fluctuations, with moderate flexibility observed in loop regions.

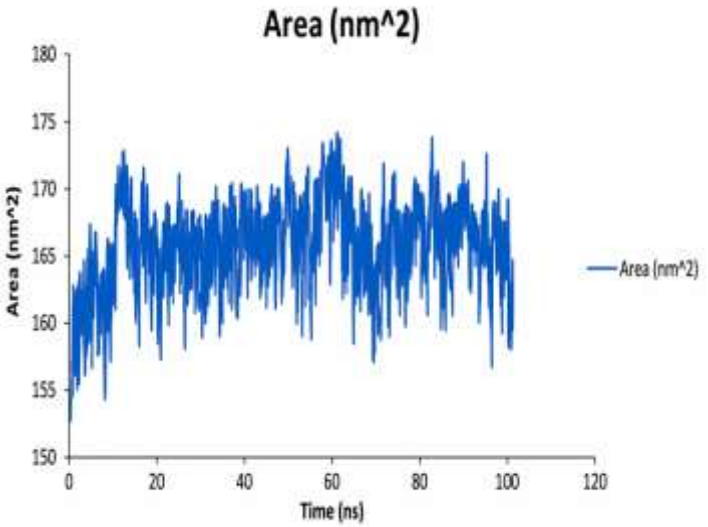

Fig.3.3 SASA analysis of the Abacavir–nsP3 complex demonstrating variations in solvent exposure during the simulation.

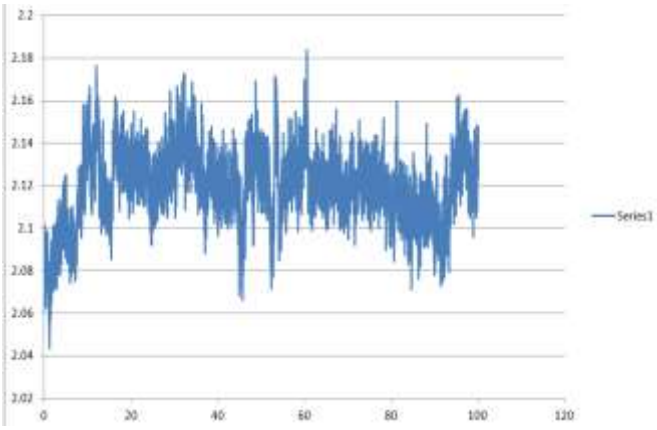

Fig.3.4. Radius of gyration (Rg) plot of the Abacavir–nsP3 complex reflecting the compactness and structural stability of the protein–ligand system.

In summary, this comparative molecular dynamics analysis shows that though Abacavir was observed to stably interact with the nsP3 protein, we are also demonstrating that the docked phytochemicals α-carotene, β-sitosterol, oleanolic acid and lupeol appeared more structurally stable; less fluctuant and more robustly engaged within the active site. These results reinforce the docking results and highlight selected phytochemicals as promising CHIKV nsP3 protein inhibitors.

3.3 ADMET Analysis

In silico ADMET prediction tools are used to analyse the pharmacokinetics and toxicity properties of selected phytochemicals, which provide insight into the pharmacophore suitability, allowing further optimization. Among the derivatives screened, nine phytochemicals showed good pharmacokinetic behavior with good adherence to ADMET features. Based on the GI absorption and bioavailability variables, such as, Lipinski's rule that include drug-likeness, the data showed that Kaempferol, Quercetin, and gallic acid do not cross any rules (Table 2). They were found to be very good with higher GI absorption scores and a reasonable value (Qaddir et al., 2018). These features indicate high oral bioavailability and potential drugability. On the other hand, many of the highest affinity compounds, such as α-carotene, β-sitosterol, and lupeol, were found to exhibit low solubility in water and several Lipinski violations due to their larger size either because of excessive lipophilicity or reduced polar surface area. These characteristics can increase the hydrophobic interactions in the protein binding pocket but may potentially limit systemic absorption and bioavailability. The majority of the individual compounds, such as chebulic acid, gallactaric acid, and lupeol showed poor gastrointestinal absorption with several Lipinski's rule violations. This could be associated with their relatively high molecular mass, hydrogen bond acceptors and donor's number, as well as their high TPSA, which can reduce membrane permeability and/or bioavailability. Not surprisingly, the compounds with an ADMET profile amenable to potential development were nicotinic acid and more so myristic acid (both showed a GI-score for gastrointestinal absorption that was high, with a bioavailability score of ~0.85; both containing high permeability across the blood- brain barrier). However, low binding affinity limits their therapeutic effectiveness on nsP3. The Toxicity Prediction Analysis revealed a good safety profile: non-cytotoxic and non-carcinogenic (Table 3). However compounds did show putative immunotoxicity and/or mutagenicity that would require experimental validation (Shamim et al., 2025). In conclusion, the ADMET analysis demonstrated an important trade-off between target binding potencies and pharmacokinetic characteristics desirable for drug candidates, indicating a strong provisional notion that finding a balance in compound features will be critical to future drug development efforts.

Table 2. Showing ADME Analysis of selected phytochemicals.

Sr. No.	Phyto compound name	CID	Lipid Solubility LogP	Water Solubility	BBB Permeability	PgpS	Gasto-intestinal Absorption	Bio availibility Score	NHBA	NHBD	TPSA (Å2)	Lipinski's rule of five
1.	Alpha carotene	6419725	10	Water insolublle	No	Yes	High	0.55	0	0	0.00	Yes, (0 violations)
2.	Ascorbic acid	54670067	1.5 to −2.0	Highly soluble	No	No	Moderate to high	0.55	1	4	107	Yes, (0 violations)

3.	Chebulic acid	72284	-0.67	Soluble in water	No	No	Low	0.11	11	6	198	No, (3 violations)
4.	Gallic acid	370	0.21	Very soluble	No	No	High	0.56	5	4	97.99	Yes, (0 violations)
5.	Beta sitosterol	222284	5.05	Poorly soluble	No	No	Low	0.55	1	1	20.23	No,(3 violations)
6.	Galactaric acid	3037582	-3 to -3.5	Highly soluble	No	No	Low	0.55	2	1	10.3	Yes, (1 violations)
7.	Kaempferol	5280863	1.70	Soluble	No	No	High	0.55	6	4	111	Yes, (0 violations)
8.	Leucodelphidin	440835	0.73	Soluble	No	No	Low	0.55	8	7	140	No, (2 violations)
9.	Linoleic acid	5280450	6-7	Poorly soluble in water	No	No	Low	0.11	2	1	37	Yes, (0 violations)
10.	Lupeol	259846	4.72	Poorly soluble	No	No	Low	0.55	1	1	20.23	Yes, (1 violations)
11.	Nicotinic acid	938	0.86	Very soluble	Yes	No	High	0.85	3	1	50.19	Yes, (0 violations)
12.	Myristic acid	11005	5-6	Poorly soluble	Yes	No	High	0.85	2	1	37.30	Yes, (0 violations)
13.	Oleanolic acid	10494	3.94	Poorly soluble	No	No	Low	0.55	3	2	57.53	Yes, (1 violations)
14.	Oleic acid	445639	4.01	Poorly soluble	No	No	High	0.85	2	1	37	Yes, (0 violations)
15.	Furosin	10416810	3.32	Poorly soluble	No	Yes	Low	0.17	19	10	316	No,(3 violations)
16.	Astragalin	5282102	1.29	Soluble	No	No	Low	0.17	11	7	190	No, (2 violations)
17.	Corilagin	73568	−0.5 to 0.5	Highly soluble	No	Yes	Low	0.17	12	8	195	No, (Multiple violations)
18.	Nitric acid	944	−2.0 to −2.5	Highly soluble	No	No	Very low	-	1	1	54	-

19.	Ellagic acid	5281855	1.0 to 1.3	Low to moderate	No	Yes	Low	0.55	8	4	141	Yes, (0 violations)
20.	Quercetin	5280343	1.5–2.0	Poorly soluble in water	No	Yes	High	0.55	7	5	131	Yes, (0 violations)
21.	Abacavir	441300	1.2-1.5	Moderate soluble	Yes	No	High	0.55	4	2	68.5	Yes, (0 violations)

Abbreviations: NHBD = Number of H-bond donors, NHBA = Number of H-bond acceptors, KP(SP) = log Kp (skin permeability), TPSA = Topological Polar Surface Area.

Table 3: Showing In Silico Toxicity Assessment of Phytocompounds Using ProTox-II.

Sr. No.	Phytocompound name	CID	Hepatotoxicity	Carcinogenicity	Immunotoxicity	Mutagenicity	Cytotoxicity
1.	Abacavir	441300	Active,(0.77)	Active, (0.51)	Inactive, (0.59)	Inactive, (0.58)	Inactive, (0.76)
2.	Alpha-carotene	6419725	Inactive,(0.85)	Inactive, (0.86)	Inactive, (0.73)	Active, (0.71)	Inactive, (0.81)
3.	Ascorbic acid	54670067	Inactive, (0.86)	Inactive,(0.92)	Inactive, (0.99)	Inactive, (0.87)	Inactive, (0.65)
4.	Astragalin	5282102	Inactive, (0.82)	Inactive,(0.85)	Inactive, (0.64)	Inactive, (0.76)	Inactive,(0.69)
5.	Ellagic acid	5281855	Inactive, (0.83)	Inactive,(0.59)	Inactive, (0.81)	Inactive, (0.84)	Inactive, (0.90)
6.	Beta- sitosterol	222284	Inactive, (0.87)	Inactive, (0.60)	Active, (0.99)	Inactive, (0.98)	Inactive,(0.94)
7.	Chebulic acid	71308174	Inactive, (0.79)	Inactive, (0.61)	Inactive, (0.94)	Inactive, (0.57)	Inactive, 0.77
8.	Corilagin	73568	Inactive, (0.85)	Inactive, (0.72)	Active, (0.72)	Inactive, (0.56)	Inactive, (0.62)
9.	Galactaric acid	3037582	Inactive, (0.93)	Inactive, (0.66)	Inactive, (0.99)	Inactive, (0.98)	Inactive, (0.74)
10.	Furosin	10416810	Inactive, (0.75)	Inactive, (0.64)	Active, (0.98)	Inactive, (0.56)	Inactive,(0.71)
11.	Gallic acid	370	Inactive, (0.61)	Active, (0.56)	Inactive, (0.99)	Inactive, (0.94)	Inactive, (0.91)
12.	Kaempferol	5280863	Inactive, (0.68)	Inactive, (0.72)	Inactive, (0.96)	Inactive, (0.52)	Inactive, (0.98)
13.	Leucodelphidin	440835	Inactive, (0.71)	Active, (0.64)	Active, (0.70)	Inactive, (0.52)	Inactive, (0.95)
14.	Linoleic acid	5280450	Inactive, (0.55)	Inactive, (0.64)	Inactive, (0.96)	Inactive, (1.0)	Inactive, (0.71)
15.	Lupeol	259846	Inactive, (0.91)	Inactive, (0.63)	Active, (0.57)	Inactive, (0.95)	Inactive, (0.97)
16.	Nicotinic acid	938	Active, (0.80)	Inactive, (0.95)	Inactive, (0.99)	Inactive, (0.99)	Inactive,(0.77)
17.	Nitric acid	944	Inactive, (0.82)	Inactive, (0.66)	Inactive, (0.99)	Inactive, (0.52)	Inactive, (0.75)
18.	Oleanolic acid	10494	Active, (0.52)	Active, (0.57)	Active, (0.79)	Inactive, (0.85)	Inactive, (0.99)
19.	Myristic acid	11005	Inactive, (0.52)	Inactive, (0.63)	Inactive, (0.99)	Inactive, (1.0)	Inactive,(0.74)

20.	Oleic acid	445639	Inactive, (0.55)	Inactive,(0.64)	Inactive, (0.99)	Inactive, (1)	Inactive,(0.71)
21.	Quercetin	5280343	Inactive, (0.69)	Active, (0.68)	Inactive, (0.87)	Active,(0.51)	Inactive, (0.99)

4. DISCUSSION

This approach led to a data-driven virtual screening study that combines in silico binding analysis, docking simulation analysis, and ADME profiling to investigate the phytochemicals derived from Emblica officinalis as Chikungunya virus nsP3 protein inhibitors. The nsP3 protein is important for viral replication, RNA synthesis, and host–virus interactions, making it a good antiviral target (Kumar et al., 2020; Rodriguez et al., 2024). However, even though nsP3 plays a critical functional role, it has not been as widely studied as other viral proteins like nsP2. Abacavir (−6.63 kcal/mol) served as the positive control; however, several screened phytochemicals showed significantly stronger binding affinities. In particular, α-carotene (−11.22 kcal/mol), β-sitosterol, oleanolic acid, and lupeol exhibited much lower (more favorable) binding energies compared to Abacavir, suggesting a higher predicted affinity for the nsP3 active site. These differences in docking scores indicate that these phytochemicals may form more stable protein–ligand complexes than the reference drug under the same computational conditions. This corroborates previous observations reporting that terpenoids and sterols have high antiviral activity because of their hydrophobic properties and ability to fit into nonpolar residues within protein binding pockets (Rahman et al., 2021; Salehi et al., 2019, Al-rooqi et al., 2023). The abundance of hydrophobic residues, such as Trp, Tyr, Leu, and Pro in the nsP3 active site likely also allows these lipophilic ligands to be stably accommodated. The increased binding affinity for hydrophobic ligands is mainly explained by the fact that the nsP3 binding pocket is highly hydrophobic. There are nonpolar residues such as Trp, Tyr, Leu, and Pro in high density in the active site that are predisposed to linking lipid compounds. The presence of hydrophobic ligands like α-carotene, β-sitosterol, and lupeol forms strong van der Waals interactions along the depth of the binding cavity, which aligns with excellent shape complementarity; however, this is often a consequence of the hydrophobic influence, in which the ordering of water molecules around the binding site is not energetically favorable upon ligand binding as this displacement leads to an increase in system entropy, stabilizing the protein–ligand complex. Additionally, hydrophobic ligands have lower desolvation energy costs with larger interaction areas, leading to more favorable binding free energy. The contributions of these factors together account for the higher docking scores achieved for lipophilic phytochemicals in this study. Such docking studies have been reported for CHIKV and other viruses, where compounds including kaempferol, lupeol and quercetin exhibited good interactions between their binding sites on viral proteins (Chaudhary et al., 2022; Lopez et al., 2022).

Their moderate binding affinities for kaempferol, quercetin and linoleic acid may be due to their ability to use two modes of interaction: hydrogen bonding and hydrophobic interactions. Flavonoids, such as kaempferol, are widely known broad-spectrum antivirals that have been reported to inhibit viral enzymes by stable hydrogen bonding and π–π stacking interaction (Kumar et al., 2013; Jo et al., 2020). Flavonoids have recorded moderate docking scores but have shown increased specificity and stability because of balanced polarity, as observed in studies released on dengue, SARS-CoV-2, and influenza proteins (Trott et al., 2010). In contrast, smaller, more polar molecules such as ascorbic acid and nicotinic acid also appear to have low binding affinities, likely because of their inability to effectively fit into the very large hydrophobic cavity involved in this binding site on nsP3. The same was not true for other polar ligands, which exhibit low affinity against nonpolar active sites due to a lack of hydrophobic stabilization (Lipinski et al., 1997), as would be expected given principles of molecular docking.

The data of the docking simulation analysis strongly supported the docking results and proved that the association of ligand-protein is structurally stable. The mean deviation (RMSD) of the backbone was stable with fluctuations and structural deviations being quite minor, in the range of 1.6–2.0 Å. This range thus confirmed that the structural integrity at equilibrium was maintained throughout the whole 100 ns timescale with different simulations. RMSD of this range is well established to represent a steady state in the MD study of a ligand-protein complex (Hollinsworth et al., 2018, Karplus et al., 2002). The few Å RMSD fluctuations of small ligand bindings within the active site demonstrate both conformational flexibility and stable binding. The RMSD profiles are comparable to those reported in MD simulation studies of crystallized protein with phytochemical complexes (Banerjee et al., 2018), and stable trajectories equilibrated belong coherently well in proportion with prolonged binding interactions to the equilibration time frame of the simulation system. Comprehensive Rg and SASA analysis also indicated that the ligand-protein complex remained stable during simulation time. The values of Rg are stable at all the simulation time frames which is indicative of global folding and compactness to nsP3 when ligand was present. This suggest that the interaction of ligand compounds does not destabilize protein structure but rather stabilizes its conformation (Bissantz et al. 2008). Consequently, SASA analysis showed no major atypical variations suggesting that the protein did not experience any extensive expansion or contraction of conformational states. This is particularly relevant, since the best-ranked ligands including α-carotene and β-sitosterol, are highly hydrophobic. Their confinement in the nonpolar cavity of nsP3 probably reduces solvent exposure and provides complex stability via hydrophobic rather than hydrogen bonding (Durrant et al., 2011). This is additionally verified because there were no intramolecular hydrogen bonds during the simulation process. Both of these findings collectively indicate that hydrophobic interactions are the predominant contributing factor to stabilizing nsP3–ligand complexes, while overall structural scaffolding of the protein is maintained throughout the simulation.

The information gained from ADME analysis provides insight into the pharmacokinetic profiles associated with the modeled compound structures. High-affinity ligands α-carotene, β-sitosterol, and lupeol did not exhibit good water solubility, and they also violated multiple Lipinski rules (Lipinski et al., 2012), which are related to their lipophilic

characteristics. This is well-documented for terpenoids and sterols of high-affinity binding but with poor oral bioavailability and absorption (Veber et al., 2002). These compounds might require structural modifications or formulation strategies to achieve better pharmacokinetic properties. Kaempferol and gallic acid are strong candidates for advancement to clinical trials; however, any benefits should be qualified in terms of the limitations associated with computational approaches like ligand–protein docking, post-docking analysis, and in silico ADME prediction that were used here (Di et al., 2015; Nemiche et al., 2022).

5. CONCLUSION

So in the current study, molecular docking, molecular dynamics simulation and ADME profiling were applied to evaluate inhibitory potentials of selected phytochemicals isolated from Emblica officinalis as potential drug targets against Chikungunya nsP3 protein. Among these, α-carotene,β-sitosterol, oleanolic acid and lupeol exhibited high affinity orientations of these compounds. The results of stable MD and docking scores suggest stable binding of these compounds in the nsP3 active pocket trajectories. Further consistency was provided by the radius of gyration and SASA profiles, which showed that despite the binding exerts a conformational perturbation there is an overall preservation of compactness in complex proteins. However, a problem with many of these high affinity compounds is there pharmacokinetics — in particular solubility and Lipinski's criteria (ADME) based violations. Quercetin, kaempferol and gallic acid, on the other hand, showed composite profiles with moderate binding energy equivalent to or better than the best natural products, incorporating drug-likeness and pharmacokinetics. Such studies underscore the crucial tradeoff between binding affinity and pharmacokinetic optimization in the process of antiviral drug design. Our findings provide potential nsP3 phytochemical candidate inhibitors through computational modeling for analysis. Moreover in comparison with Abacavir (the standard drug), selected phytochemicals have a high potential to be effective against CHIKV nsP3 protein. But these results are based on in-silico predictions that deserve follow-up validation by binding free energy calculations and structure validation by advanced experimental methods like biological and cell culture–based assays. The consequences of this study will result in growth in the portfolio of plant-based antiviral agents and may aid in potential novel therapeutic avenues in CHIKV infection. The integration of traditional medicinal knowledge with computational approaches highlights the potential of Emblica officinalis as a valuable source of antiviral lead compounds

Acknowledgement

We are grateful to the University Grant Commission (UGC) (Ref. No. 231610196715) for providing financial assistance to Ripu Daman in the form of JRF. We are also grateful to Centre for Bioinformatics, Maharishi Dayanad University for providing necessary infrastructure Laboratory facilities to conduct dry lab analysis.The infrastructural and academic support provided by the host institution is also gratefully acknowledged.

Competing interest

The authors declare that there are no competing interests regarding the publication of this paper.

REFERENCES

- Ali, A., Akhtar, N., Khan, B. A., Khan, M. S., Rasul, A., Zaman, S. U., & Ali, L. (2012). Acacia nilotica: A plant of multipurpose medicinal uses. Journal of Medicinal Plants Research, **6**(9), 1492–1496.
- Al-Rooqi, M. M., Mughal, E. U., Raja, Q. A., Hussein, E. M., Naeem, N., Sadiq, A., & Ahmed, S. A. (2023). Flavonoids and related privileged scaffolds as potential urease inhibitors: A review. RSC Advances, **13**(5), 3210–3233.
- Ashfaq, U. A., Mumtaz, A., ul Qamar, T., & Fatima, T. (2013). MAPS database: Medicinal plant activities, phytochemical and structural database. Bioinformation, **9**(19), 993.
- Azmal, M., Hossen, M. S., Shohan, M. N. H., Taqui, R., Malik, A., & Ghosh, A. (2024). A computational approach to identify phytochemicals as potential inhibitor of acetylcholinesterase: Molecular docking, ADME profiling and molecular dynamics simulations. PLoS One, **19**(6), e0304490.
- Banerjee, P., Eckert, A. O., Schrey, A. K., & Preissner, R. (2018). ProTox-II: A webserver for the prediction of toxicity of chemicals. Nucleic Acids Research, **46**(W1), W257–W263.
- Binder, K., Horbach, J., Kob, W., Paul, W., & Varnik, F. (2004). Molecular dynamics simulations. Journal of Physics: Condensed Matter, **16**(5), S429–S453.
- Bissantz, C., Kuhn, B., & Stahl, M. (2010). A medicinal chemist's guide to molecular interactions. Journal of Medicinal Chemistry, **53**(14), 5061–5084.
- Bowers, K. J., Albright, B. J., Yin, L., Daughton, W., Roytershteyn, V., Bergen, B., & Kwan, T. J. (2009). Advances in petascale kinetic plasma simulation with VPIC and Roadrunner. Journal of Physics: Conference Series, **180**, 012055.
- Chaudhary, M., & Sehgal, D. (2022). In silico identification of natural antiviral compounds as a potential inhibitor of chikungunya virus non-structural protein 3 macrodomain. Journal of Biomolecular Structure and Dynamics, **40**(22), 11560–11570.
- Daina, A., Michielin, O., & Zoete, V. (2017). SwissADME: A free web tool to evaluate pharmacokinetics, drug-likeness and medicinal chemistry friendliness of small molecules. Scientific Reports, **7**, 42717.
- Di, L., & Kerns, E. H. (2015). Drug-like properties: Concepts, structure design and methods from ADME to toxicity optimization. Academic Press.
- Durrant, J. D., & McCammon, J. A. (2011). Molecular dynamics simulations and drug discovery. BMC Biology, **9**, 71.

- Dutta, S., Burkhardt, K., Bluhm, W. F., & Berman, H. M. (2005). Using the tools and resources of the RCSB protein data bank. Current Protocols in Bioinformatics, **9**(1), 1–9.
- Fagre, A. C., & Kading, R. C. (2019). Can bats serve as reservoirs for arboviruses? Viruses, **11**(3), 215.
- Feinstein, W. P., & Brylinski, M. (2015). Calculating an optimal box size for ligand docking and virtual screening. Journal of Cheminformatics, **7**, 18.
- Ferreira, L. G., Dos Santos, R. N., Oliva, G., & Andricopulo, A. D. (2015). Molecular docking and structure-based drug design strategies. Molecules, **20**(7), 13384–13421.
- Gaire, B. P., & Subedi, L. (2014). Phytochemistry, pharmacology and medicinal properties of Phyllanthus emblica Linn. Chinese Journal of Integrative Medicine.
- Hamed, A. R., Abdel-Azim, N. S., Shams, K. A., & Hammouda, F. M. (2019). Targeting multidrug resistance in cancer by natural chemosensitizers. Bulletin of the National Research Centre, **43**, 8.
- Hollingsworth, S. A., & Dror, R. O. (2018). Molecular dynamics simulation for all. Neuron, **99**(6), 1129–1143.
- Jo, S., Kim, S., Shin, D. H., & Kim, M. S. (2020). Inhibition of SARS-CoV 3CL protease by flavonoids. Journal of Enzyme Inhibition and Medicinal Chemistry, **35**(1), 145–151.
- Karplus, M., & McCammon, J. A. (2002). Molecular dynamics simulations of biomolecules. Nature Structural Biology, **9**(9), 646–652.
- Kim, S. (2021). Exploring chemical information in PubChem. Current Protocols, **1**(8), e217.
- Kim, S., Chen, J., Cheng, T., Gindulyte, A., He, J., He, S., Bolton, E. E. (2021). PubChem in 2021. Nucleic Acids Research, **49**(D1), D1388–D1395.
- Kumar, D., Meena, M. K., Kumari, K., Patel, R., Jayaraj, A., & Singh, P. (2020). In-silico prediction of novel drug-target complex of nsp3 of CHIKV. Heliyon, **6**(8).
- Kumar, S., & Pandey, A. K. (2013). Chemistry and biological activities of flavonoids. The Scientific World Journal, 162750.
- Lipinski, C. A., Lombardo, F., Dominy, B. W., & Feeney, P. J. (1997). Experimental approaches to estimate solubility and permeability. Advanced Drug Delivery Reviews, **23**, 3–25.
- Lipinski, C. A., Lombardo, F., Dominy, B. W., & Feeney, P. J. (2012). Molecular properties influencing oral bioavailability. Advanced Drug Delivery Reviews, **64**, 4–17.
- Lobanov, M. Y., Bogatyreva, N. S., & Galzitskaya, O. V. (2008). Radius of gyration as an indicator of protein compactness. Molecular Biology, **42**(4), 623–628.
- Meng, X. Y., Zhang, H. X., Mezei, M., & Cui, M. (2011). Molecular docking: A powerful approach. Current Computer-Aided Drug Design, **7**(2), 146–157.
- Metz, S. W., Gardner, J., Geertsema, C., Le, T. T., Goh, L., Vlak, J. M., & Pijlman, G. P. (2013). Chikungunya virus-like particle vaccine. PLoS Neglected Tropical Diseases, **7**(3), e2124.
- Morris, G. M., Goodsell, D. S., Halliday, R. S., Huey, R., Hart, W. E., Belew, R. K., & Olson, A. J. (1998). Automated docking using Lamarckian genetic algorithm. Journal of Computational Chemistry, **19**, 1639–1662.
- Morris, G. M., Huey, R., Lindstrom, W., Sanner, M. F., Belew, R. K., Goodsell, D. S., & Olson, A. J. (2009). AutoDock4 and AutoDockTools4. Journal of Computational Chemistry, **30**(16), 2785–2791.
- Rahman, M. M., Biswas, S., Islam, K. J., Paul, A. S., Mahato, S. K., Ali, M. A., & Halim, M. A. (2021). Antiviral phytochemicals against dengue virus. Computers in Biology and Medicine, **134**, 104492.
- Rallabandi, H. R., Mekapogu, M., Natesan, K., Saindane, M., Dhupal, M., Swamy, M. K., & Vasamsetti, B. M. K. (2020). Computational methods in phytocompound drug discovery. Springer.
- Sharma, P., Joshi, T., Joshi, T., Chandra, S., & Tamta, S. (2021). Molecular dynamics simulation of phytochemicals. Journal of Biomolecular Structure and Dynamics, **39**(17), 6524–6538.
- Shanmugaraj, B., & Balasubramanian, H. (2026). Epidemiological trends and policy interventions in the context of chikungunya in India. Discover Public Health, 23(1), 199.
- Trott, O., & Olson, A. J. (2010). AutoDock Vina. Journal of Computational Chemistry, **31**(2), 455–461.
- Veber, D. F., Johnson, S. R., Cheng, H. Y., Smith, B. R., Ward, K. W., & Kopple, K. D. (2002). Molecular properties influencing oral bioavailability. Journal of Medicinal Chemistry, **45**(12), 2615–2623.
- Weaver, S. C., & Lecuit, M. (2015). Chikungunya virus global spread. New England Journal of Medicine, **372**(13), 1231–1239.
- Zaid, A., Gérardin, P., Taylor, A., Mostafavi, H., Malvy, D., & Mahalingam, S. (2018). Chikungunya arthritis mechanisms. Arthritis & Rheumatology, **70**(4), 484–495.
- Zhang, J., Li, H., Zhang, Y., Huang, J., Ren, L., Zhang, C., & Zhang, Y. (2025). Computational toxicology in drug discovery. Briefings in Bioinformatics, **26**(5), bbaf533.